iJRASET
International Journal For Research in Applied Science and Engineering Technology

INTERNATIONAL JOURNAL FOR RESEARCH

IN APPLIED SCIENCE & ENGINEERING TECHNOLOGY

Volume: 6 **Issue:** III **Month of publication:** March 2018

DOI: http://doi.org/10.22214/ijraset.2018.3169

www.ijraset.com

Call: 08813907089 | E-mail ID: ijraset@gmail.com

International Journal for Research in Applied Science & Engineering Technology (IJRASET)
ISSN: 2321-9653; IC Value: 45.98; SJ Impact Factor: 6.887
Volume 6 Issue III, March 2018- Available at www.ijraset.com

Effect of Chemically Synthesis compared to Biosynthesized CeO_2 NP_S using Aqueous Extract of Momordica Charantia

B. Anand[1], A. Muthuvel[2], V. Mohana[3], S. Anandhi[4], M.Pavithra[5]
[1]*Department of Physics, Government Arts and Sciences College, C. Mutlur, Chidambaram, India*
[2]*PG Research Department of physics TBML College, Poraiyar, India*
[3]*Annamalai University, Annamalai Nagar. India*

Abstract: ***In the present work, chemically synthesis compared to Biosynthesized CeO_2 NP_S using aqueous extract of M. charantia (15 mL) concentrations. Influence of the synthesized products were characterized by Ultra violet–Vis spectroscopy, X-ray diffraction, Fourier transform infrared, Scanning electron microscopy and, UV–visible spectrometry study revealed surface plasmon resonance at 276 nm, The XRD patterns show the cubic phase and average particle sizes are 15 nm, The functional groups and band area of the samples were established by FT-IR spectroscopy the presence of both leaf extract and CeO_2 NPs. The surface morphologies analysis has been hexagonal quartzite structure confirmed from SEM. The present Bio - CeO_2 NPs nanoparticles suggests that have the great potential applications on various industrial and medical fields of research***
Keywords: Chem- CeO_2 NPs, Bio - CeO_2 NPs, SEM, FT-IR

I. INTRODUCTION

In recent years the development of green processes for the synthesis ofmetal and metal oxide nanoparticles is evolving into an important branch of nanotechnology. Nanotechnology is the study and design of machines on the molecular and atomic size Nanopartcles are of great interest due to their extremely atom-like behavior due to large surface energy area to volume ratio, high fraction of surface atoms and wide gap between valence and conduction band when divided to near atomic level which lead to both physical and chemical differences in their properties of nanopartcles catalytic activity, thermal and electrical conductivity, biological and satirical properties and optical characteristics compared to the bulk materials [1]. The characteristic properties of nanoparticles exhibit completely new or improved properties based on specific such as increased surface area, distribution, size and morphology are different and improved when compared with larger particles of the bulk counterparts. Metal and metal oxide nanoparticles particles are extensively exploited because of their unique physical properties, chemical reactivity and potential applications in various research areas such as antimicrobial, magnetic, electronic, catalytic, medication, water treatment, air filtration and photocatalysis to eliminate various pollutants and hazardous dyes [2].Amongst the metal oxide nanoparticles, cerium oxide nanoparticles have drawn interest of a lot of researchers for their unique optical and chemical behaviors which can be simply tuned by changing the morphology. Within the large family of metal oxide nanoparticles, cerium oxide nanoparticles have been utilised in a variety of cutting edge applications like electronics, communication, sensor, cosmetics, environmental safety, biology and medicinal industry [3]. In addition cerium oxide nanoparticles have a tremendous potential in biological applications like biological sensing, biological labelling, gene delivery, drug delivery and nanomedicines. A number of approaches are available for the production of metal nanoparticles such as chemical, physical and biological utilize less time for synthesizing large quintets of nanopartcles, they require toxic chemicals as capping agents to maintain stability, thus leading to toxicity in the environment. Keeping this in consideration of biosynthesis of nanoparticles using plants is emerging as an eco-friendly alternative, as plant extract mediated biosynthesis reaction is cost-e□ectve [4] CeO_2 NPs has been synthesized in a plethora of shapes with a nano size controlled manner in view of targeted applicatons, photonic and spintronics devices, optical, electrical, cosmetics, agriculture, anti-cancer and anti-microbial Currently, a number of researchers are interested in using CeO_2 NPs to diagnose medical disorders.

Momordica charantia L. (Cucurbitaceae) is known as a kind of edible vegetable in Asian countries, such as China, Bangladesh, India, Japan, and Korea. It has also been extensively used as a traditional Chinese medicinal plant to prevent and treat toothache, diarrhea, diabetes and furuncle. As a medicinal plant, bitter melon is used in the treatment of several diseases or conditions including diabetes, HIV, viral infections, cancer, inflammation, ulcers, and sepsis. The whole plant Momordica charantia contains saponins, traces of alkaloids, flavonoids, proanthocyanidin, apigenin and phytosterols, In the leaves larger amounts of saponins and

©IJRASET (UGC Approved Journal): All Rights are Reserved

alkaloids were found, also (+) -pinitol, apigenin, luteolin and Chrysoeriol, The mother tincture contains a relatively higher amount of flavonoids than the plant [5]. Many processes have reported the synthesis of CeO_2 nanoparticles using plant extracts based production of nanomaterials has wide range of application such as antimicrobial property by [6-7]. Against these backdrops in this present study aimed at the Chemically synthesis of CeO_2 NPs compared to biosynthesized CeO_2 NP_S using aqueous extract of M. charantia to investigate the biomolecules responsible for synthesis of CeO_2 NPs and finally to evaluate antibacterial activity to the best of our knowledge, the use of M. charantia leaf extract. Has not been reported so far for the biosynthesis of noble nanoparticles, such as CeO_2 NPs. The stability of chemically synthesis of CeO_2 NPs compared to biosynthesized CeO_2 NP_S using leaf extract was evaluated and characterized by UV-DRS spectrum, , XRD, FT-IR, SEM,

II. MATERIALS AND METHODS

A. Materials

Fresh leaves of M. charantia (Figure 1). Have been collected from rural places of Chidambaram, Cuddalure District, Tamil Nadu, India. Cerium chloride heptahydrate ($CeCl_3.7H_2O$) (99.9%) was procured from Sigma-Aldrich, Bangalore Chemicals for this study. All other reagents utilized in the response had been of analytical grade with highest purity. All aqueous remedies have been ready producing use of deionized water.

Figure 1. Photograph of M. charantia

B. Preparation Of Leaf Extract

The fresh and healthful leaves of M. charantia have been washed many times with de-ionized water to remove the dust particles on their surface. A healthful and undamaged leaf of M. charantia 10 grams of leaf was finely cut and stirred with 100 mL of de-ionized water at 85°C for 25 min, using microwave irradiation. The leaf extract was allowed to great and filtered through Whatman No.1 filter paper. The filtered leaf extract was used for even more experiments as reducing agent and stabilizer of synthesis nanoparticles.

C. Chemically Synthesis of CeO_2 NPs

CeO_2 NPs were synthesized by direct precipitation method using cerium nitrate and KOH as precursors. In this work, the aqueous solution (3.45g) of Cerium chloride heptahydrate ($CeCl_3.7H_2O$) and the solution (0.4 M) of KOH were prepared with deionized water, respectively. The KOH solution was slowly added into zinc nitrate solution at room temperature under vigorous stirring, which resulted in the formation of a white suspension. The white product was centrifuged at 5000 rpm for 20 min and washed three times with distilled water, and washed with absolute alcohol at last. The obtained product was calcined at 500°C in air atmosphere for 3 hr.

D. Biosynthesized CeO_2 NP_S using M. Charantia leaf extract

The synthesis of CeO_2 NPs involved the mixing of aliquot amounts of cerium nitrate and M. charantia leaf extract in water. The M. charantia leaf extract (15 mL) was added to 10 0 mL of 1 mM ($CeCl_3.7H_2O$) aqueous boiled solution and kept at boiling condition for 20 min to get the colloids. The ($CeCl_3.7H_2O$)) and aqueous leaf extract M. charantia show any color change primarily

©IJRASET (UGC Approved Journal): All Rights are Reserved

confirmed the production of CeO_2 NPs by a visual color change from turned light green in color and the reaction rate was completed after 24 h. The material was powered using a mortar and pestle so, that got a fine powder, which is easy for further characterizations.

E. Characterization of synthesized CeO_2 NPs

The UV–Vis reflectance spectra UV- Vis reflectance evaluation was carried out by a computer managed in a wavelength selection from 200–800 cm^{-1}. The biosynthesized cerium nanoparticles was monitored by the crystalline form of CeO_2 NPs stability and particle dimension distribution have been characterized X-ray diffraction (XRD) measurements of the *M. charantia* leaf extract broth decreased CeO_2 NPs have been carried out at 2v. The presence of functional groups and the binding residence of the CeO_2 NPs were established by Fourier transform infrared spectroscopy (FT-IR) have been recorded in the selection of 400–4000 cm^{-1}. Using SEM approach, the dimension, form, and morphology of the CeO_2 NPs nanoparticles have been examined, the SEM was applied at an accelerating voltage of 25 kV

III. RESULTS AND DISCUSSIONS

A. Optical Properties

The absorption spectra of the Chem- CeO_2 NPs and Bio- CeO_2 NPs were studied to investigate the effect of optical properties. Figure 2 shows the UV–Visible absorption spectra of the prepared samples. The absorption spectrum of the Chem- CeO_2 NPs shows an excitonic absorption edge at 285 nm. The absorption peak of the Biosynthesized using *M. charantia* leaf extract CeO_2 NPs were shifted to 276 nm, respectively, the transparency in visible range of the CeO_2 NPs decreases. The changes in optical transmittance are because of *M. charantia* leaf extract concentrations and the UV–visible spectra the sharpness of the absorption peak is dependent on the concentration of leaf extract, thus being sharper with a higher concentration of leaf extract [8]

B. The Band Gap Energy

The band gap energy (Eg) of Chem- CeO_2 NPs and Bio- CeO_2 NPs samples were calculated from the wavelength value corresponding to the intersection point of the vertical and horizontal part of the spectrum determined using the equation [9].

$$\mathbf{E} = \mathbf{h}\nu = h.c/\lambda \quad \ldots\ldots\ldots\ldots\ldots\ldots\ldots\ldots\ldots\ldots 1$$

Where C is the speed of light in vacuum (3 x 10^8 m/s), λ is the wave length of the λ=c/ν (λ=403 nm), h is Plank's constant (6.626 x 10^{-34} J.s), ν is the frequency

The band gap energy calculated to be 4.03 eV and 3.84 eV for the samples of Chem- CeO_2 NPs, and Biosynthesized using *M.* charantia leaf extract CeO_2 NPs samples Figure 3. Respectively. It can be seen that a linear decrease in the band gap from 4.03 to 3.84 eV and also found to decrease in energy gap of CeO_2 with M. charantia leaf extract using CeO_2 NPs. Therefore, UV–Vis analysis reveals that M. charantia leaf extract causes decrease in band gap energy of Bio- CeO_2 NPs. The changes in optical band gap values may be due to the change of crystal structure of Bio- CeO_2 NPs

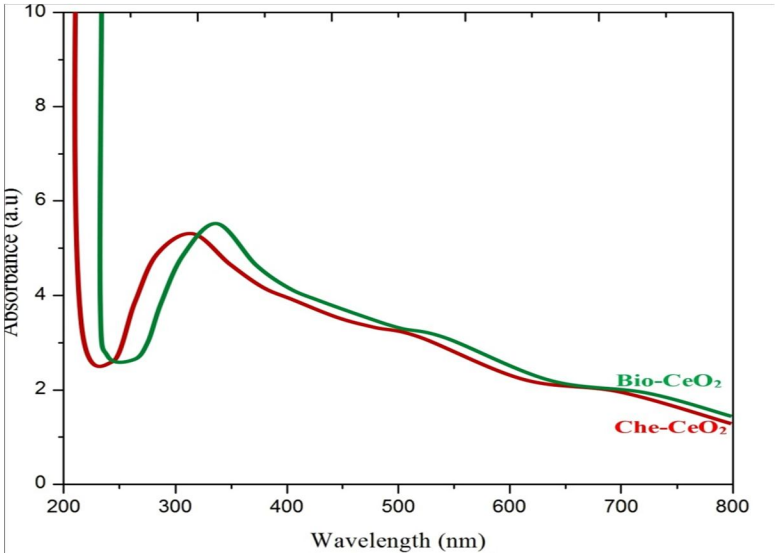

Figure.2. UV-Visible absorption spectrum of Chem-CeO_2 and Bio- CeO_2 nanoparticles

©IJRASET (UGC Approved Journal): All Rights are Reserved

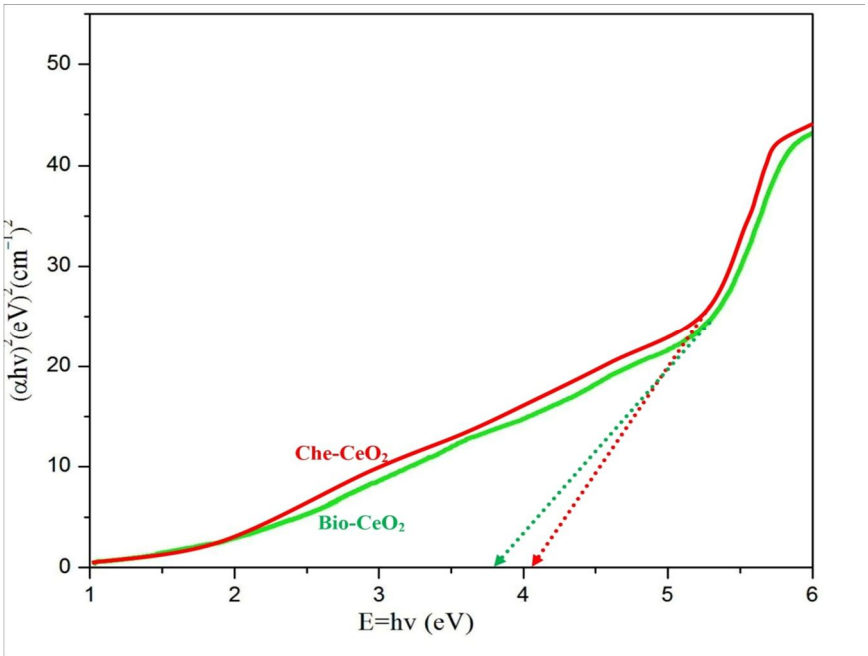

Figure 3. Band gap energy of Chem-CeO_2 and Bio- CeO_2 nanoparticles

C. XRD Analysis

The power X-ray diffraction patterns (XRD) of Chem- CeO_2 NPs, and Biosynthesized CeO_2 NPs using *M. charantia* extract. The diffraction peaks in the XRD pattern consist of the diffraction peaks of Chem- CeO_2 NPs and Bio- CeO_2 NPs in the prepared product, several diffraction peaks appeared and all the diffraction pattern obtained are well indexed to the Face-centered cubic-fluorite structure of CeO_2 (JCPDS 43-1002) in Figure.4 The diffraction peaks with 2θ = 28.08°, 32.25°, 47.26°, 55.66°, 62.06°, 69.23°, 76.07°, and 79.70° correspond to the crystal plans of (111), (200), (220), (311), (222), (400), (331) and (422) of Biosynthesized CeO_2 nanoparticles using M. charantia leaf extract were confirmed the Face-centered cubic-fluorite structure respectively [10]. Here, no other impurity peaks are detected in the XRD patterns indicating that all products are rather purity of the nanoparticles formation. The high intensity peaks (111) and (220) have been used to estimate the average crystalline sizes of Chem.-ZnO NPs, and Biosynthesized using M. charantia leaf extract of sample with the help of Scherer equation [11]

$$D = \frac{K\lambda}{\beta \cos\theta} \quad \ldots\ldots\ldots\ldots\ldots (2)$$

Where, K- is constant (0.9) λ- is the wavelength of the CuKa radiation (0.154056 nm), and θ is the peak position and β is the Full Width at Half Maximum (FWHM).

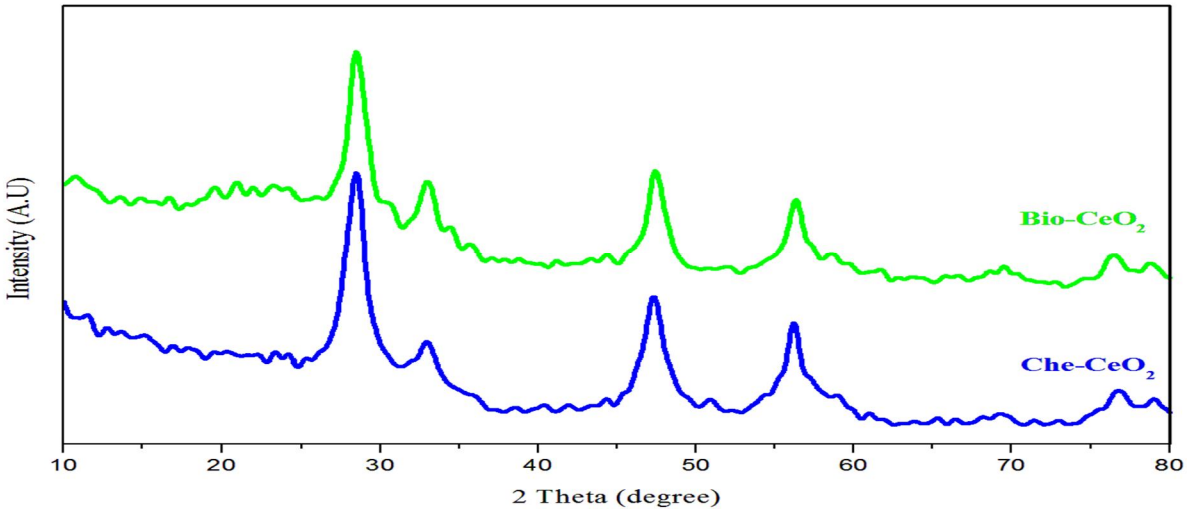

Figure 4. X-ray diffraction pattern of Chem-CeO_2 and Bio- CeO_2 nanoparticles

©IJRASET (UGC Approved Journal): All Rights are Reserved

The mean crystallite size of Chem - CeO_2 NPs, is 45 nm as shown in Table 1, whereas of Biosynthesized using M. charantia leaf extract the estimated sizes are 15 nm, respectively as shown in Tables 2. The reduction of particle size from 45 to 15 nm on of M. charantia leaf extract using Bio- CeO_2 NPs this reveals its optimum level, a facile biosynthesis method to synthesize the CeO_2 NPs and effect of calcinations in this result agrees literature. No apparent diffraction peaks of any other minerals can be detected in the XRD patterns. There are no apparent characteristic peaks of M. charantia leaf extract uing Bio- CeO_2 NPs can be observed, indicating that the M. charantia has immersed into the CeO_2 NPs nanoparticles matrixes. In order to get nanocrystallite sizes increases, these final results confirmed the M. charantia has been leaf extract effectively in CeO_2 NPs matrixes and possibly enhanced the crystallinity, and crystallinity is extremely relevant to the full width at half maxima (FWHM) value further, the XRD profile shows that CeO_2 NPs are strongly crystallized with a preferred (111) orientation, which has been observed by other authors.

D. FTIR Analysis

The functional groups responsible for the in order to identify the possible reducing and stabilizing bio molecules using FT-IR analysis. FT-IR analysis was carried through the wavenumber range from 400 to 4000 cm^{-1} using KBr pellet method at room temperature. Figure 3.7 shows for Chem – CeO_2 NPs and Biosynthesized CeO_2 NPs using *M. charantia* leaf extract respectively. The absorption bands at 3490.76, 2998.95, 2608, 2263, 1507, 1274.23, 1120 and 796 cm^{-1} in *M. charantia* leaf extract. The peak appeared 1507.71 cm^{-1} represent the water and hydroxyl stretches [12] and 3490.76 cm^{-1} may be assigned to the bending vibrational modes of the absorbed H_2O and surface O-H stretching modes, respectively, the intensive band 1274.23 respresents N-O stretch due to the presence of nitrate, C-H stretching absorption around 2998.95 cm^{-1}, a C-O-C stretching absorption around 1164 cm^{-1}[13], the absorption band at wavenumber 796.09 cm^{-1}represent the Ce-O stretch. We confirmed the formation of nanopaeticles using FT-IR, the FT-IR spectrum wavenumber indicate the participation of saponins, traces of alkaloids, flavonoids, proanthocyanidin, apigenin and phytosterols and aliphatic amines in bioreduction reactions.

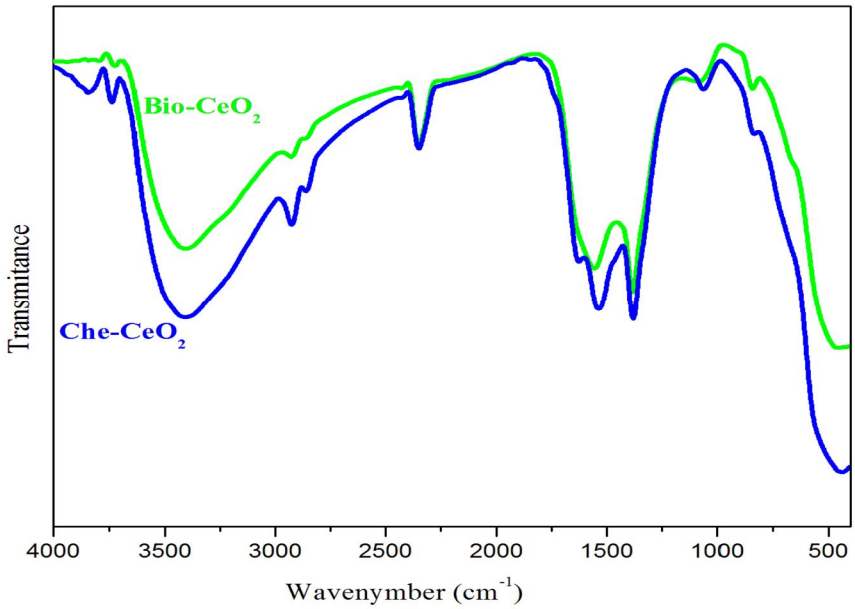

Figure 4. FT-IR spectrum of Chem-CeO_2 and Bio- CeO_2 nanoparticles

E. SEM Analysis

The morphology and microstructure of Chem – CeO_2 NPs, and Biosynthesized CeO_2 NPs using *M. charantia* leaf extract products were examined by SEM. The study of SEM gave a clear indication and dispersion of Chem- CeO_2 NPs and Bio- CeO_2 NPs as shown in Figure (5-6), respectively. The distinctive images demonstrated that the particles were Face-centered cubic-fluorite structure with some surface agglomeration. This result indicates that the variation Chem-CeO_2 NPs and Bio- CeO_2 NPs. The SEM analysis confirms the XRD analysis. Also, the substrate surface is well covered with grains that are almost uniformly distributed over the surface. The M. charantia leaf extract compositions as shows the smooth surface morphology and grain size of the particles controlled by M. charantia leaf extract using Bio- CeO_2 NPs. Increasing order of M. charantia leaf extract concentrations contributes to more regular structure and hexagonal and clear formation of Bio- CeO_2 NPs. Further, this good agreement between FT-IR and XRD studies.

©IJRASET (UGC Approved Journal): All Rights are Reserved

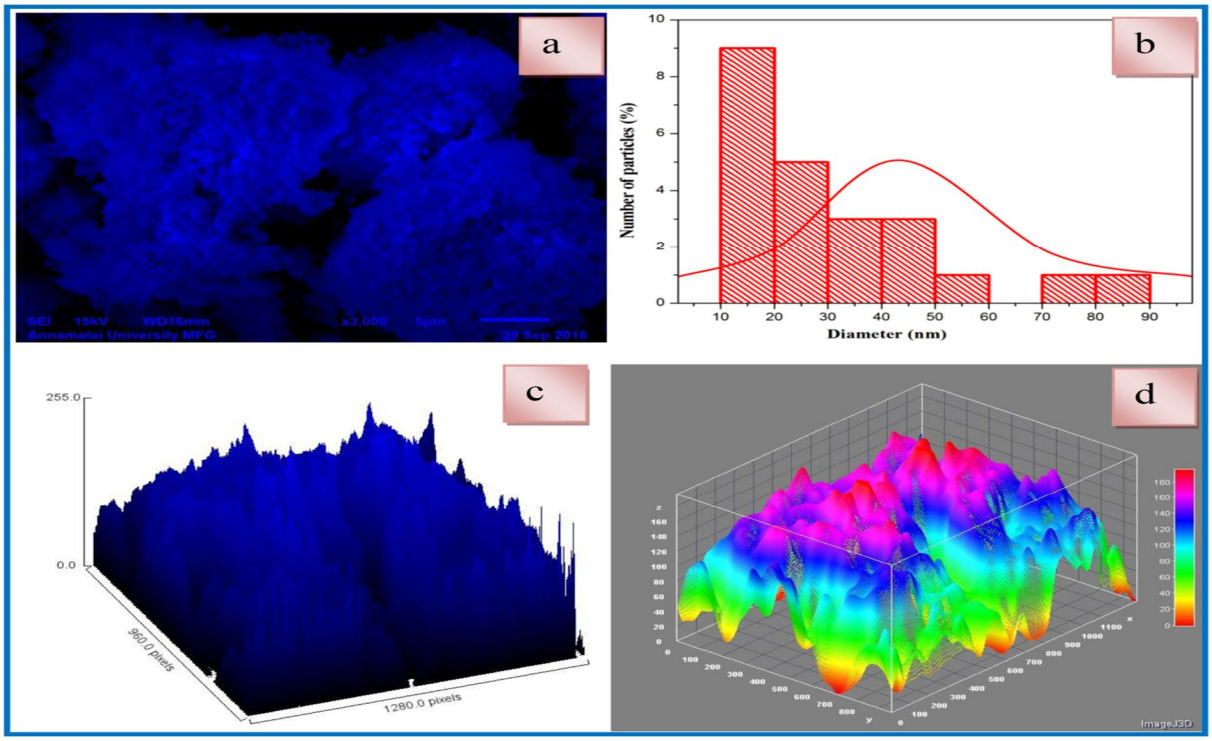

Figure. 5. a) SEM image b) size distribution histograms c) Surface occupancy plot and d) Surface profile analysis in Chem-CeO_2 nanoparticles

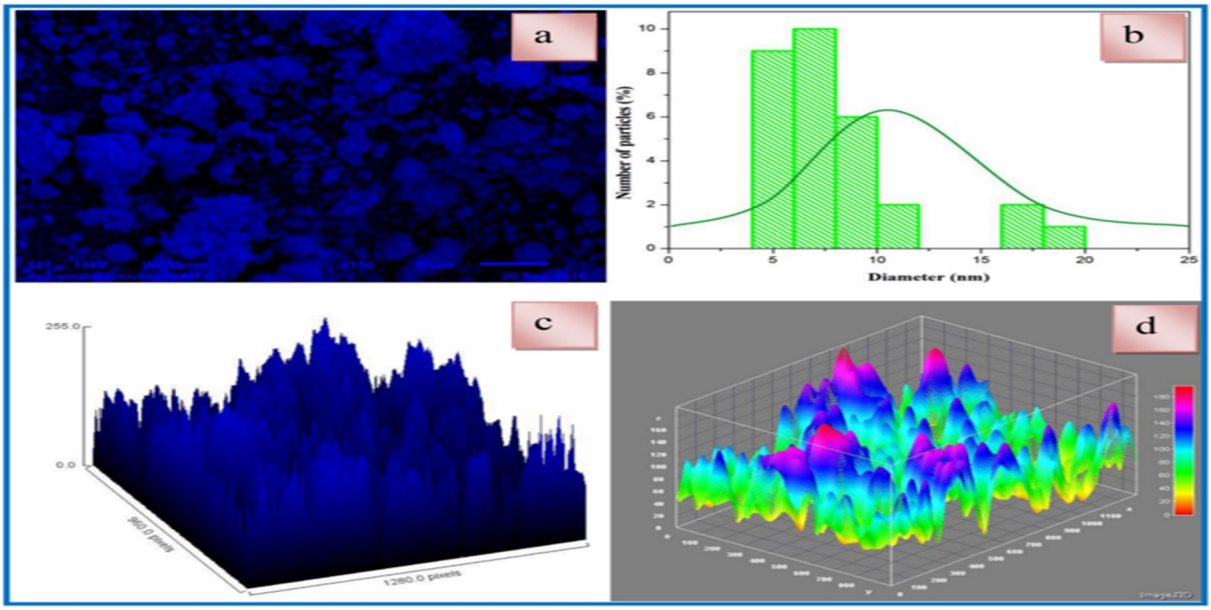

Figure 6 a) SEM image b) size distribution histograms c) Surface occupancy plot and d) Surface profile analysis in Bio -CeO_2 nanoparticles

IV. CONCLUSION

The metal oxide nanoparticles has friendly with environment emerged as a low cost, simpler and better choice than Biosynthesized methods. The biosynthesized CeO_2 Nps from Cerium nitrate solution using M. charantia leaf extract and the Bio CeO_2 Nps were found to be the band gaps were identified by UV-Visible spectroscopy and were found to be XRD almost Face-centered cubic-fluorite structure with particle size around 15 nm. FT-IR shows that peak at the absorption band at wavenumber 796.09 cm^{-}

©IJRASET (UGC Approved Journal): All Rights are Reserved

[1]represent the Ce-O stretch which confirms formation of cerium oxide nanoparticles. Therefore, the present study has been useful and helpful for the applications of nano-drugs design, medicinal, potential applications for various semiconductors and industrial fields.

Table 1 Comparison of 2θ, d-spacing, β and Cosθ values of Chem CeO_2-NPs at wavelength k = 0.15308 nm

Position (2θ)	d-spacing	hkl	FWHM (β)	Cosθ	Average particles size
28.05	2.70386	100	0.58390	0.9539	
32.06	2.34229	002	0.56140	0.9443	
47.03	2.65743	101	0.51750	0.8834	
55.09	1.52682	102	0.48530	0.8394	
62.08	1.45415	110	0.43830	0.8234	45nm
69.04	1.35246	103	0.78560	0.8856	
76.04	1.28675	112	0.86759	0.9867	
79.01	1.24356	202	1.18670	0.9876	

Table 1 Comparison of 2θ, d-spacing, β and Cosθ values of Bio- CeO_2-NPs at wavelength k = 0.15308 nm

Position (2θ)	d-spacing	hkl	FWHM (β)	Cosθ	Average particles size
28.08	2.77860	100	0.65678	0.9076	
32.25	2.66754	002	0.59878	0.9203	
47.26	2.00689	101	0.40235	0.8574	
55.66	1.48763	102	0.46783	0.8574	
62.06	1.98671	110	0.40088	0.8500	15nm
69.23	1.00856	103	0.75470	0.8116	
76.07	1.20987	112	0.99865	0.9997	
79.70	1.26086	202	1.19087	0.9320	

REFERENCES

[1] S. Yedurkar, C. Maurya, and P. Mahanwar, Biosynthesis of Zinc Oxide Nanoparticles Using Ixora Coccinea Leaf Extract—A Green Approach, Open Journal of Synthesis Theory and Applications, 05, 01, 1–14, 2016.
[2] S. Chakrabarti and B. Dutta, Photocatalytic degradation of model textile dyes in wastewater using ZnO as semiconductor catalyst," Journal of Hazardous Materials, vol. 112, 3, 269–278, 2004.
[3] J. W. Rasmussen, E. Martinez, P. Louka, and D. G. Wingett, Zinc oxide nanoparticles for selective destruction of tumor cells and potential for drug delivery applications, Expert Opinion on Drug Delivery, 7, 9, 1063–1077, 2010.
[4] S. Suwanboon and P. Amornpitoksuk, Structural, Optical and Photocatalytic Properties of ZnO Nanoparticles Prepared by Precipitation Method, Advanced Materials Research, 979, 163–166, 2014.
[5] G. Nahler, Committee for Veterinary Medicinal Products (CVMP), Dictionary of Pharmaceutical Medicine, 32–32, 2009.
[6] F. Schwabe, R. Schulin, L. K. Limbach, W. Stark, D. Bürge, and B. Nowack, Influence of two types of organic matter on interaction of CeO2 nanoparticles with plants in hydroponic culture," Chemosphere, 91, 4, 512–520, 2013.
[7] Q. Maqbool, "Green-synthesised cerium oxide nanostructures (CeO2-NS) show excellent biocompatibility for phyto-cultures as compared to silver nanostructures (Ag-NS)," RSC Advances, 7, 89, 56575–56585, 2017.
[8] A. Saxena, R. M. Tripathi, F. Zafar, and P. Singh, Green synthesis of silver nanoparticles using aqueous solution of Ficus benghalensis leaf extract and characterization of their antibacterial activity, Materials Letters, 67, 1, 91–94, 2012.
[9] S. Sivakumar, A. Venkatesan, P. Soundhirarajan, and C. P. Khatiwada, Thermal, structural, functional, optical and magnetic studies of pure and Ba doped CdO nanoparticles, Spectrochimica Acta Part A: Molecular and Biomolecular Spectroscopy, 151, 760–772,2015.
[10] K. Kalimuthu, R. Suresh Babu, D. Venkataraman, M. Bilal, and S. Gurunathan, "Biosynthesis of silver nanocrystals by Bacillus licheniformis," Colloids and Surfaces B: Biointerfaces, 65, 1, 150–153, 2008.
[11] S. Sivakumar, A. Venkatesan, P. Soundhirarajan, and C. P. Khatiwada, Synthesis, characterizations and anti-bacterial activities of pure and Ag doped CdO nanoparticles by chemical precipitation method, Spectrochimica Acta Part A: Molecular and Biomolecular Spectroscopy,136, 751–1759, 2015.
[12] N. F. Hamedani, A. R. Mahjoub, A. A. khodadadi, and Y. Mortazavi, CeO2 doped ZnO flower-like nanostructure sensor selective to ethanol in presence of CO and CH4, Sensors and Actuators B: Chemical, 169,67–73,2012.
[13] C. Li, S. Shu, R. Chen, B. Chen, and W. Dong, "Functionalization of electrospun nanofibers of natural cotton cellulose by cerium dioxide nanoparticles for ultraviolet protection," Journal of Applied Polymer Science, vol. 130, no. 3, pp. 1524–1529, Apr. 2013.

©IJRASET (UGC Approved Journal): All Rights are Reserved

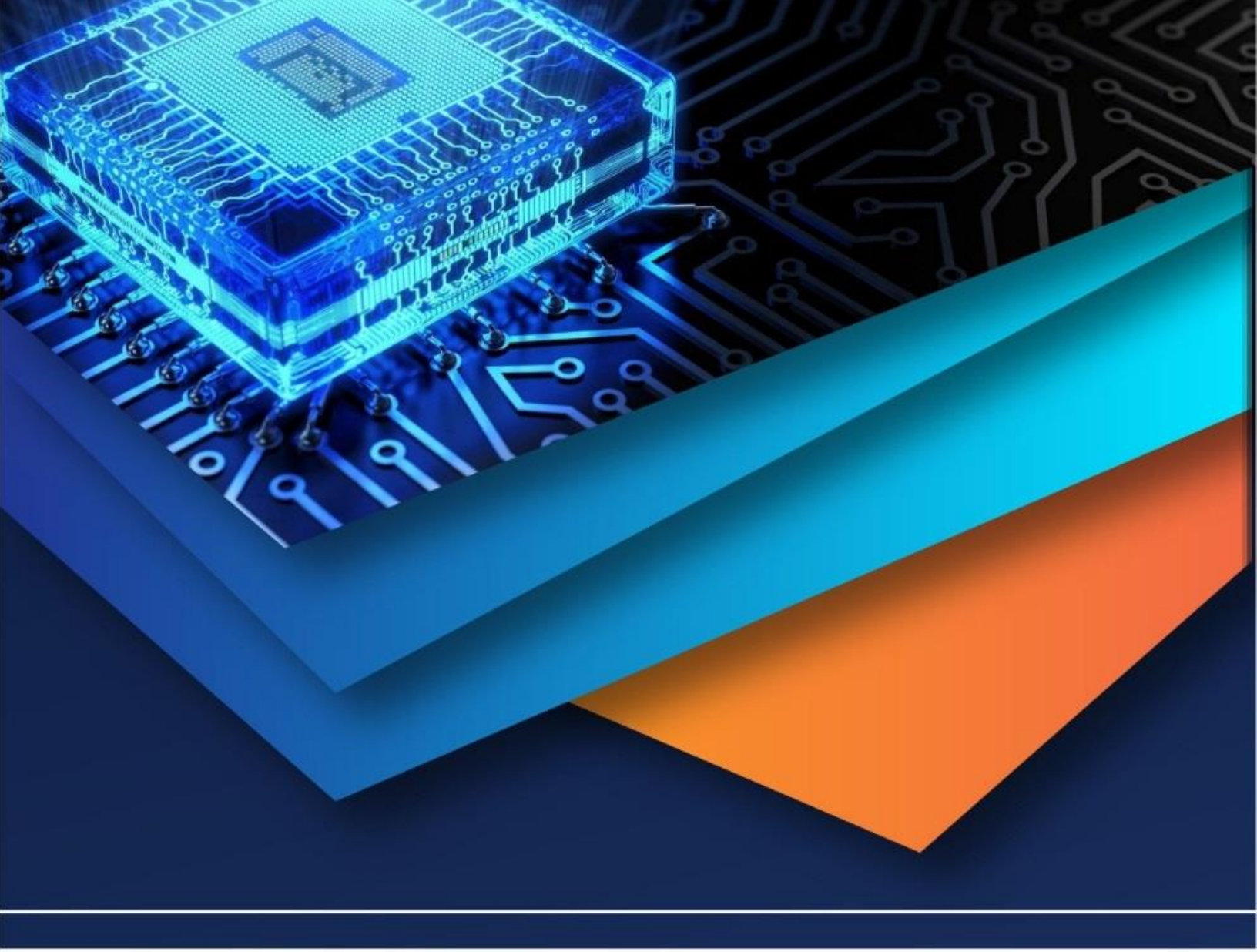

10.22214/IJRASET

45.98

IMPACT FACTOR: 7.129

IMPACT FACTOR: 7.429

INTERNATIONAL JOURNAL FOR RESEARCH

IN APPLIED SCIENCE & ENGINEERING TECHNOLOGY

Call : 08813907089 (24*7 Support on Whatsapp)